

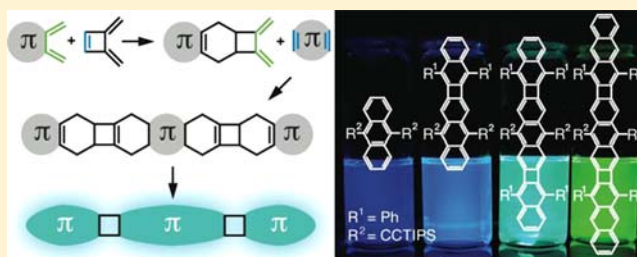
Synthesis and Optical Properties of Phenylene-Containing Oligoacenes

Rebecca R. Parkhurst and Timothy M. Swager*

Department of Chemistry, Massachusetts Institute of Technology, 77 Massachusetts Avenue, Cambridge, Massachusetts 02139, United States

S Supporting Information

ABSTRACT: Synthesis of a new class of fully unsaturated ladder structures, phenylene-containing oligoacenes (POAs), using 3,4-bis(methylene)cyclobutene as a building block for sequential Diels–Alder reactions is described. The geometric effects of strain and energetic cost of antiaromaticity can be observed via the optical and electrochemical properties of the reported compounds. The resulting shape-persistent ladder structures contain neighboring chromophores that are partially electronically isolated from one another while still undergoing a reduction in the band gap of the material.



INTRODUCTION

The promise of organic electronics to enable creation of inexpensive, flexible, and multifunctional devices¹ is presently limited by access to stable high-performance materials. One strategy to develop such materials is to create extended rigid aromatic systems that promote delocalization and minimize energetic disorder in the electronic states. Among the polycyclic aromatic hydrocarbons (PAHs), acenes, defined as linearly annelated arenes with the fewest number of rings containing Clar sextets,² are considered one of the most important candidates for high-performance organic semiconductors (Figure 1a).

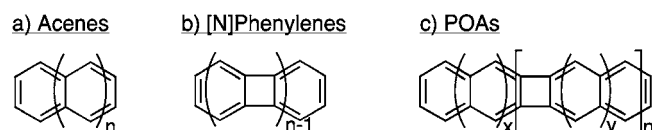


Figure 1. General structure of (a) acenes, (b) [N]phenylenes, and (c) phenylene-containing oligoacenes (POAs).

A natural strategy to create higher charge mobilities in an organic material is to increase the spatial electronic delocalization in the constituent molecular building blocks. However, as the length of the acene increases, the reduction in aromaticity also causes a rapid decrease in the HOMO–LUMO gap and the chemical stability of these materials becomes problematic. The higher acene homologues do appear to have improved electronic properties, such as increasing charge mobility, decreasing reorganization energy, and a predicted decrease in exciton binding energy. This final property is appealing for solar cell applications, where recently the unique ability of acenes to undergo singlet fission has been of interest

as a method of creating two dissociated charge carriers from a single photon.³

Close relatives to the acenes are the [N]phenylenes, a family of PAHs wherein benzene rings are fused together by four-membered rings, resulting in a ladder structure with alternating aromatic and antiaromatic character (Figure 1b).⁴ Molecules of this family have classically been synthesized via the [2 + 2 + 2] cycloaddition methodology developed largely by Vollhardt et al. It has been demonstrated both experimentally and theoretically that the π bonds in these systems tend to localize within the six-membered rings so as to minimize the 4π antiaromatic character of the cyclobutadiene linkage.⁵ Recently, a dibenzannulated biphenylene framework served as key intermediate in the synthesis of the first example of [4]circulene.⁶

Analogously to the acenes, linear annulation in the [N]phenylenes correlates to a more rapidly decreasing band gap than does angular.⁷ This behavior is consistent with the theoretical prediction that, as with polyacene, [N]phenylenes of infinite length could serve as molecular wires.⁸ We report herein that antiaromatic phenylene linkages can be used in conjunction with oligoacene units to create high-stability extended, shape-persistent phenylene-containing oligoacenes (POAs) with interesting optical properties.

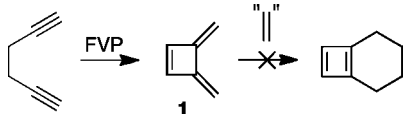
RESULTS AND DISCUSSION

Diels–Alder Reactivity of 3,4-Bis(methylene)-cyclobutene. The synthesis reported herein relies on the unique Diels–Alder reactivity of 3,4-bis(methylene)-cyclobutene (**1**), generated by flash vacuum pyrolysis of 1,5-hexadiyne according to the published procedure (Scheme 1).⁹

Received: May 6, 2012

Published: September 5, 2012

Scheme 1. Synthesis of 3,4-Bis(methylene)cyclobutene (1) by Flash Vacuum Pyrolysis (FVP)^a



^aCompound 1 is not reactive as a Diels–Alder diene.

Although the exocyclic methylene groups of **1** are locked in the desired *s*-cis conformation, it is not reactive as a Diels–Alder diene as the resulting product would contain cyclobutadiene. However, we have shown that initial reaction of the endocyclic double bond with a diene such as 1,3-diphenylisobenzofuran (Scheme 2) is facile and selective. This reaction, in turn, generates a single isomer of **2a**, which is reactive as a Diels–Alder diene. A second Diels–Alder reaction with 1,4-naphthoquinone (NQ) yields a single isomer of polycyclic **3**.

The stereoselectivity of each Diels–Alder reaction has been confirmed by both 2D NMR of **2** (Figure 2) and X-ray crystallography of **3** (Figure 3a). Although Diels–Alder reactions of isobenzofurans tend to result in a mixture of isomers,¹⁰ the initial reaction in this case is selective for the exo product, consistent with previous reports by Kaupp et al.¹¹ Long-range couplings (J^3)¹² between H^a and carbons C1 and C2 are expected in the endo product with corresponding torsion angles of 31° and 167°, respectively, in the energy-minimized structure. These cross-peaks are not present in the heteronuclear multiple bond correlation (HMBC-NMR) spectrum, indicating formation of exo product, in which the torsion angles are 77° and 57°, respectively.

Examining the calculated LUMO of **1** (B3LYP/6-31g**, Figure 2b), secondary orbital interactions (SOI) of the orbitals on C3/4 with the diene HOMO would favor the endo transition state; however, the coefficients at this position are significantly smaller than those at C5/C6.¹³ Additionally, the geometry of the highly strained ring brings the C5/C6 molecular orbitals closer to the reaction site, causing instead an antibonding interaction in the endo transition state. In the second Diels–Alder reaction, the product results from approach of the dienophile to the less hindered side of diene **2**.

Synthesis of POAs. With **3** in hand, its fully unsaturated counterpart, compound **6**, is readily available through a series of synthetic transformations (Scheme 2). Addition of a strong

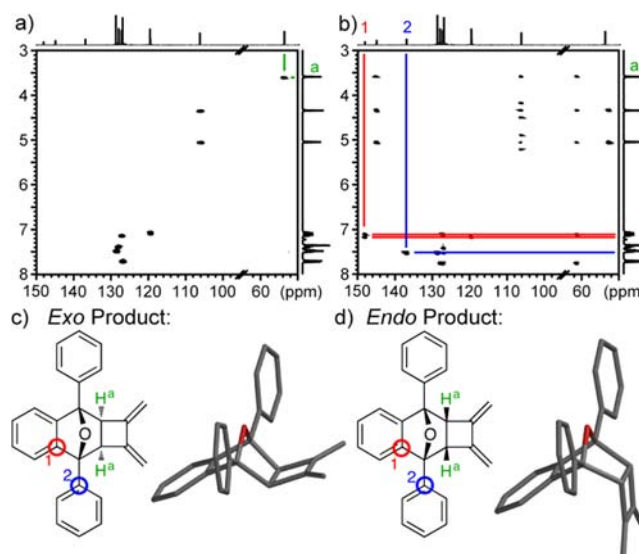


Figure 2. Determination of the stereochemistry of **2a**. (a) Heteronuclear single quantum coherence-NMR (HSQC-NMR), (b) HMBC-NMR, (c) exo product, and (d) endo product.

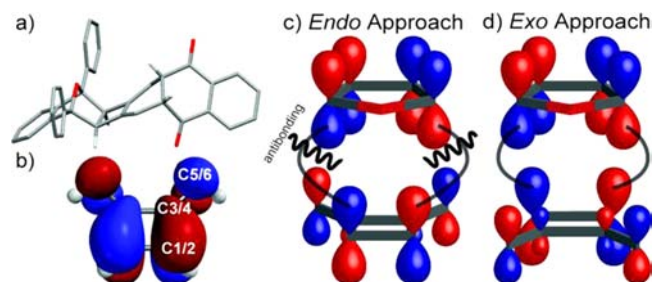
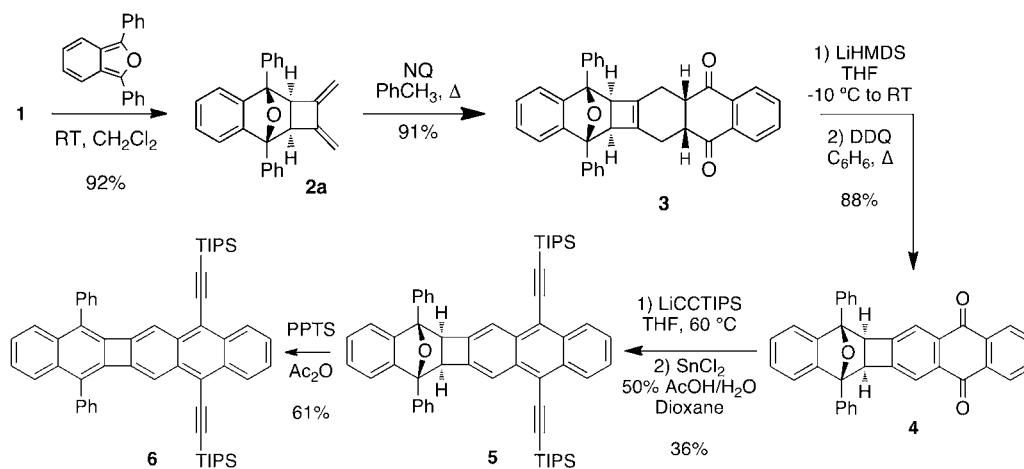


Figure 3. (a) X-ray crystal structure of **3**. (b) LUMO of **1** (B3LYP/6-31g**). (c) Endo and (d) exo approaches of **1** to a furan diene.

base such as lithium hexamethyldisilazide (LiHMDS) generates the high-energy bis-enolate, which then oxidizes to the 1,4-quinone, presumably by action of air introduced during the workup. 2,3-Dichloro-5,6-dicyano-1,4-benzoquinone (DDQ) is then used to aromatize the neighboring ring, giving compound **4** in an 88% yield over two steps (for X-ray crystal structure of **4** see Figure S5 and S6, Supporting Information). Nucleophilic

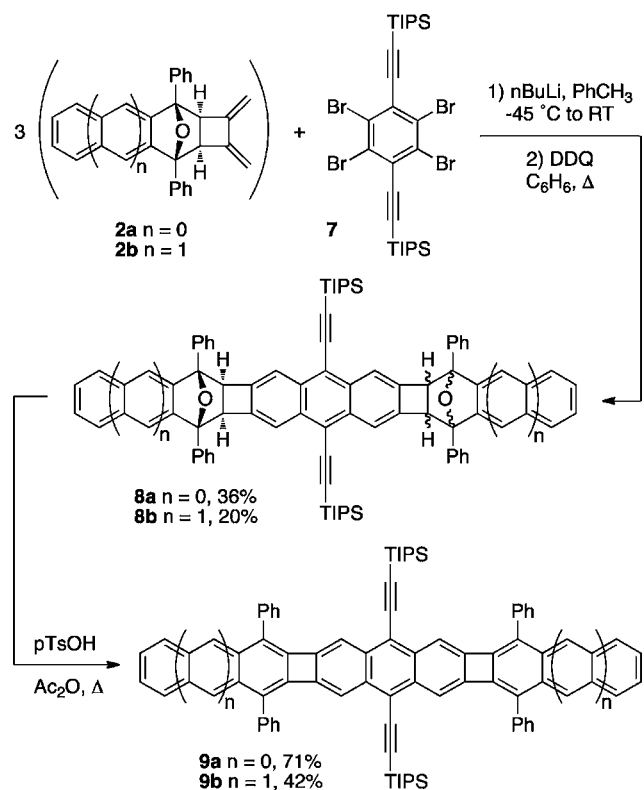
Scheme 2. Sequential Diels–Alder Reactions to Yield 3 and Synthesis of POA 6



addition of TIPS-protected lithium acetylide followed by reductive deoxygenation yields the TIPS-anthracene-containing **5**. Finally, **5** is dehydrated by pyridinium *p*-toluenesulfonate (PPTS) in acetic anhydride (Ac₂O) to give **6**. Analysis by differential scanning calorimetry (DSC) indicates the high thermal stability of POA **6** (Figure S1, Supporting Information).

On the basis of the synthetic methodology demonstrated above, molecules of this family can be extended into even larger structures (Scheme 3). 1,3-Diphenylisobenzofuran¹⁴ can be

Scheme 3. Bisaryne Diels–Alder Reaction and Aromatization To Yield POAs 9a/b



used to generate diene **2b**. Reacting a bis-functionalized dienophile with **2** results in symmetrical structures. As a bisaryne precursor, we chose to use 1,2,4,5-tetrabromo-1,6-bis(triisopropylsilyl)ethynylbenzene (**7**), synthesized via the procedure previously reported by our laboratory.¹⁵ Products from the bisaryne Diels–Alder addition of **2** with **7** were taken on to the aromatization step without further purification to yield isomeric mixtures of precursors **8a/b**. Dehydration was then carried out with *p*-toluene sulfonic acid (*p*TsOH) in acetic anhydride to give the desired POAs **9a/b**. POA **9a** also exhibits high thermal stability, and no phase changes are evident up to 400 °C via DSC. POA **9b** appears to be moderately stable in the solid state in the absence of light.

Optical and Electrochemical Properties. Analysis of the optical properties of **6** and **9a/b** as compared to those of TIPS-anthracene (TIPS-Anth)¹⁶ is shown in Figure 4. In a solution of chloroform (CHCl₃), the absorbance curve of **5** is almost identical to that of TIPS-Anth with the exception of a slightly lower energy absorption around 260 nm corresponding to the phenyl substituents (Figure S2, Supporting Information). In the case of **6**, there are two distinct absorbances: a higher energy

absorption due to the diphenylnaphthalene chromophore and a lower energy absorption ($\lambda_{\text{max}} = 464$ nm) due to the diethynyl-anthracene chromophore. The 21 nm bathochromic shift between TIPS-anthracene and compound **6** demonstrates that although the phenylene linkage limits delocalization between the two chromophores there is still sufficient communication to cause a reduction in the band gap of about 0.17 eV. A similar pattern is evident in the solution absorbance curves of **9a/b**, with a reduction in the band gap with each increase in the length of the POA.

There is a corresponding bathochromic shift in the solution emission curve of each POA. Emission quantum yields decrease within the series from TIPS-Anth ($\phi_{\text{em}} = 0.94$) to **9b** ($\phi_{\text{em}} = 0.26$). In each case the Stokes shifts are small, ranging from 2 to 5 nm, consistent with the rigid, shape-persistent nature of these materials.

In each case, the solid-state absorbance curves are characterized by only very small bathochromic shifts (ranging from 1 to 11 nm) as compared to the solution state measurements, and there is virtually no change in the vibronic structure. The small changes may indicate that electronic coupling between neighboring molecules in the solid state is not as efficient as in unsubstituted acenes.¹⁷ This feature is likely the result of the steric isolation from the pendant phenyl and TIPS groups that also create large intermolecular spacings in the crystal packing of **6** and **9a** (vide infra). The apparent weak electronic coupling between POAs and the small red shifts in the optical band gap with increasing length will likely limit the utility of these specific materials in organic photovoltaic materials.

The change in the emission spectrum of TIPS-Anth in going from solution to solid state is likewise very small. However, the case is different for POAs **6** and **9a/b**, where new large bathochromic emission features are observed. In films of POAs **6** and **9a** there appear to be two emission processes, with one resembling the unimolecular solution S₁–S₀ transitions at 477 and 514 nm, respectively. Extension of the outer acenes appears to create intermolecular actions that produce a new longer wavelength emission, and in the case of POA **9b** only the low-energy emission band (630 nm) is evident. These new features are relatively sharp and have hints of vibrational fine structure on the bathochromic side of the major peaks. As a result of this structure they do not appear to be excimer emissions. The minimal spectral changes in the absorption spectra upon going from solution to solid state are not suggestive of bulk formation of J-aggregates; however, it is possible that a small amount of a J-aggregated material is present in the film and that excitonic migration to this state produces this large Stokes-shifted material. A small band bathochromic of the absorbance spectrum of **9b** (~580 nm) supports this claim.

The ionization potential and stability of the oxidized forms of the POAs were analyzed by cyclic voltammetry (CV) (Table 1 and Figure S3, Supporting Information). The difference in the potential of the first oxidation peak (E_{ox} vs Fc/Fc⁺) of TIPS-Anth, **6**, and **9a** is quite small, decreasing from 710 mV for TIPS-Anth to 678 mV for **9a**. Therefore, the reduction in the band gap for these three species can primarily be attributed to a decreasing LUMO level, confirming oxidative stability. Although TIPS-Anth and **6** both undergo only one reversible oxidation, compound **9a** displays a second oxidation peak within the window studied. Compound **9b**, alternatively, exhibits three reversible oxidation peaks, with the first two shifted to significantly lower potentials than those previously

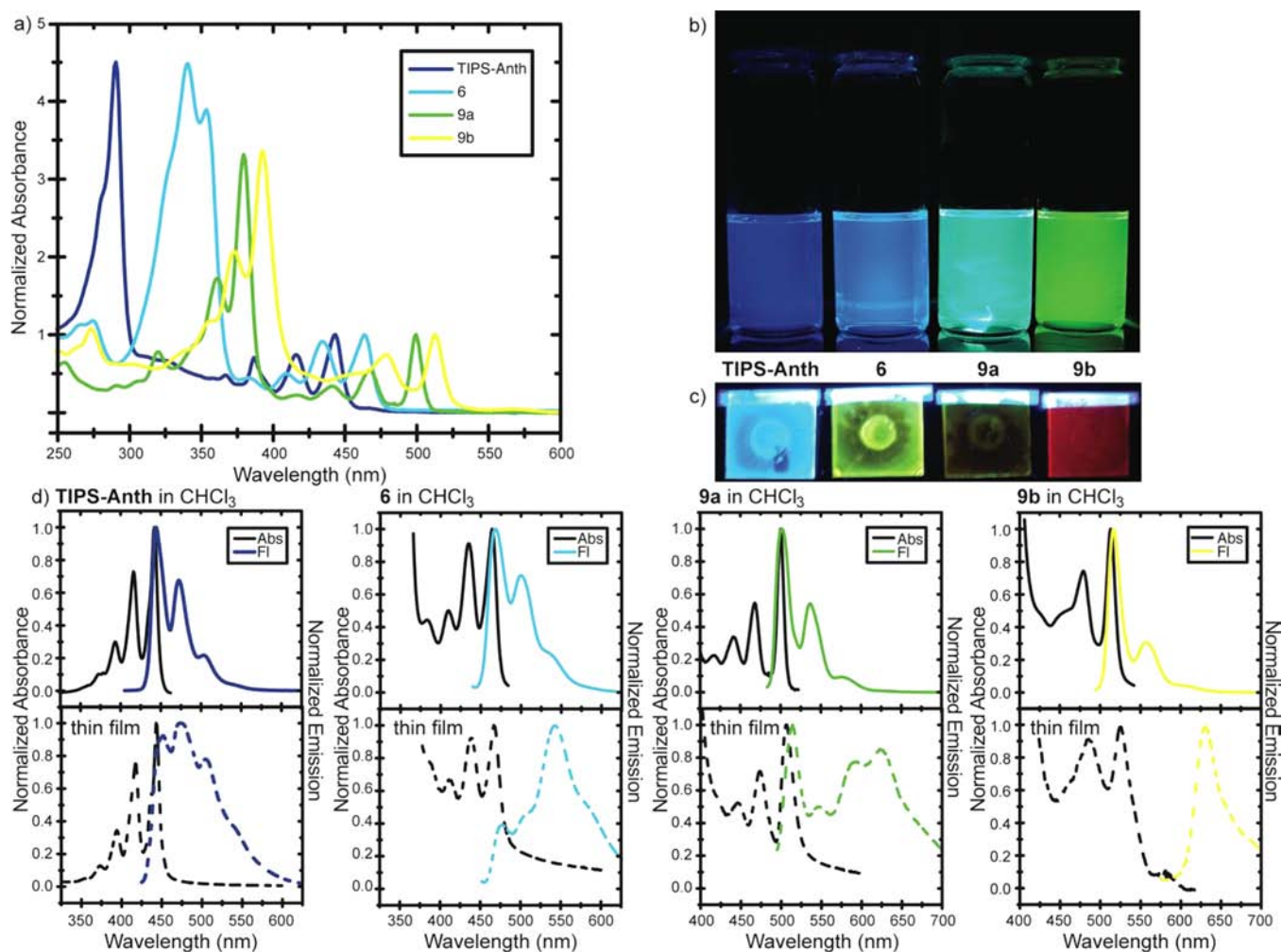


Figure 4. (a) Overlay of the absorbance curves of TIPS-Anth, 6, and 9a/b. (b) Solution and (c) solid state emission. (d) Solution state (solid line) absorbance and emission: TIPS-Anth $\lambda_{\max} = 442$ nm, $\lambda_{\text{em}} = 444$ nm, $\phi_{\text{em}} = 0.97$, $\tau = 5.04$ ns; 6 $\lambda_{\max} = 464$ nm, $\lambda_{\text{em}} = 469$ nm, $\phi_{\text{em}} = 0.69$, $\tau = 7.72$ ns; 9a $\lambda_{\max} = 500$ nm, $\lambda_{\text{em}} = 502$ nm, $\phi_{\text{em}} = 0.45$, $\tau = 5.60$ ns; 9b $\lambda_{\max} = 513$ nm, $\lambda_{\text{em}} = 517$ nm, $\phi_{\text{em}} = 0.26$, $\tau = 6.71$ ns. Solution state measurements were performed in CHCl_3 . Solid state (dotted line) absorbance and emission: TIPS-Anth $\lambda_{\max} = 443$ nm, $\lambda_{\text{em}} = 452, 473, 504$ nm; 6 $\lambda_{\max} = 467$ nm, $\lambda_{\text{em}} = 477, 543$ nm; 9a $\lambda_{\max} = 506$ nm, $\lambda_{\text{em}} = 514, 594, 623$ nm; 9b $\lambda_{\max} = 524$ nm, $\lambda_{\text{em}} = 630$ nm. Thin films were spin cast from solutions of CHCl_3 .

Table 1. Electrochemical Data for POAs

compound	E_{ox} (mV) ^a vs Fc/Fc^+	HOMO ^b (eV)	LUMO ^b (eV)	E_{g} (optical) ^c (eV)
TIPS-Anth	710	-5.42	-2.68	2.74
6	702	-5.41	-2.84	2.57
9a	678	-5.39	-2.96	2.43
9b	527	-5.24	-2.87	2.37

^aPerformed in a 0.1 M solution of TBAPF₆ in CH_2Cl_2 , Pt button electrode, scan rate 150 mV/s, ferrocene as an external standard.

^bHOMO levels were determined from E_{ox} and used in conjunction with the optical band gap to determine LUMO levels. ^cDetermined from λ_{onset} in CHCl_3 .

discussed. Consistent with these findings, 9b appears to be susceptible to slow oxidative degradation in the solution state, whereas the same was not evident in solutions of 6 and 9a.

Structural Analysis. Compounds 6 and 9a were both analyzed by X-ray crystallography (Figure S5). Examination of the bond lengths around the phenylene linkage confirms the increased localization of π bonds, with bond lengths alternating between ~ 1.44 Å exocyclic and ~ 1.36 Å endocyclic to the four-

membered ring C. Bonds linking the acenoid segments have even greater single-bond character with a bond length of 1.498 Å in each case.

As mentioned above, although theoretical studies have shown [N]phenylenes to be planar in the lowest energy conformation, crystal structures of this family of hydrocarbons have often proved to be bent, likely due to the effects of crystal packing forces on the increased flexibility of the backbone.¹⁸ In the case of 6 and 9a there are small torsion angles around the phenylene linkage ($5.60^\circ/1.31^\circ$ and $1.58^\circ/0.05^\circ$, respectively); however, the molecules are very close to planar.

For both crystals of 6 and 9a, the molecules assemble into two cofacial one-dimensional stacks with different orientations. The intermolecular distances in the crystal packing are relatively large for PAHs, 7.50 Å for 6 and 7.80 Å for 9a, likely due to the steric bulk of the side groups. There is also a shorter edge-to-face interaction between the phenyl substituents of opposing stacks of 4.89 Å for 6 and 4.19 Å for 9a.

SUMMARY

In conclusion, we reported the design and synthesis of a new class of nonbenzenoid PAHs, phenylene-containing oligo-

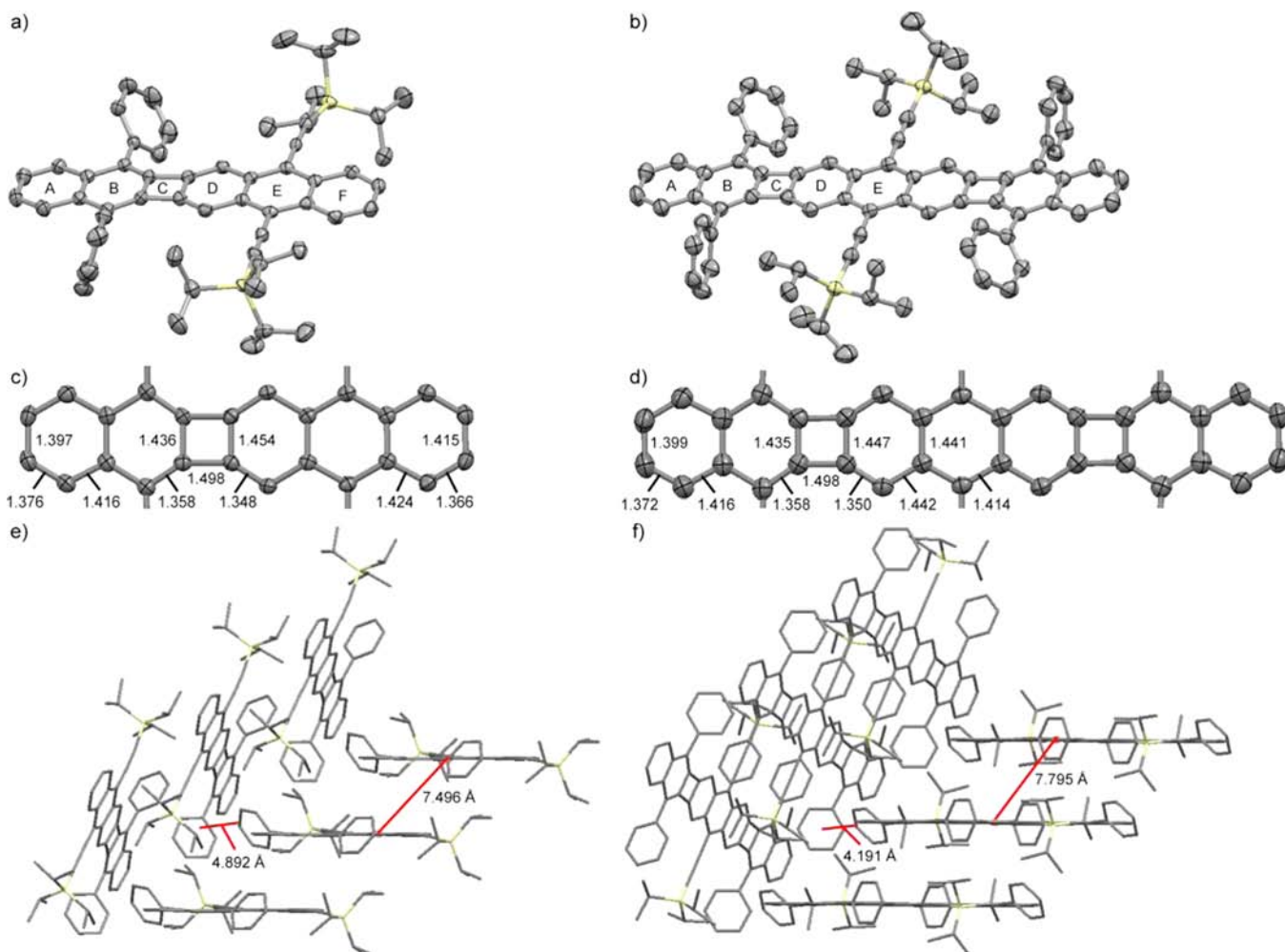


Figure 5. X-ray crystal structures of (a) **6** and (b) **9a**. Selected bond lengths (Angstroms) in (c) **6** and (d) **9a**. Crystal packing of (e) **6** and (f) **9a**.

enes. The unique reactivity of 3,4-bismethylene-cyclobutene was exploited to build ladder structures via sequential Diels–Alder reactions. The resulting POAs represent stable, shape-persistent chromophores, with band gap and quantum efficiencies that decrease as length increases. Studies on the ability of this class of molecules to participate in singlet fission are underway.

■ ASSOCIATED CONTENT

📄 Supporting Information

Experimental data including synthetic procedures, characterization data for all compounds, and additional figures. This material is available free of charge via the Internet at <http://pubs.acs.org>.

■ AUTHOR INFORMATION

Corresponding Author

E-mail: tswager@mit.edu

Notes

The authors declare no competing financial interest.

■ ACKNOWLEDGMENTS

This work was supported by the National Science Foundation DMR-1005810 and as part of the Center for Excitronics, an Energy Frontier Research Center funded by the U.S. Department of Energy, Office of Science, Office of Basic

Energy Sciences under Award Number DE-SC0001088. We thank the National Science Foundation for departmental X-ray diffraction instrumentation (CHE-0946721).

The authors thank Dr. Peter Müller and Dr. Michael Takase for collecting and solving X-ray structure data. The authors also thank Dr. Brett VanVeller for providing compound **7** for initial studies.

■ REFERENCES

- (1) Anthony, J. E. *Angew. Chem., Int. Ed.* **2008**, *47*, 452.
- (2) Ruiz-Morales, Y. *J. Phys. Chem. A* **2002**, *106*, 11283.
- (3) (a) Smith, M. B.; Michl, J. *Chem. Rev.* **2010**, *110*, 6891 and references therein. (b) Siebbeles, L. D. A. *Nat. Chem.* **2010**, *2*, 608.
- (c) Jadhav, P. J.; Mohanty, A.; Sussman, J.; Lee, J.; Baldo, M. A. *Nano Lett.* **2011**, *11*, 1495. (d) Ramanan, C.; Smeigh, A. L.; Anthony, J. E.; Marks, T. J.; Wasielewski, M. R. *J. Am. Chem. Soc.* **2011**, *134*, 386.
- (4) For a review on [N]Phenylenes, see: Miljanić, O. Š.; Vollhardt, K. P. C. In *Carbon-Rich Compounds: From Molecules to Materials*; Haley, M. M., Tykwinski, R. R., Eds.; Wiley-VCH: Weinheim, 2006; pp 140–197.
- (5) Schleifenbam, A.; Feeder, N.; Vollhardt, K. P. C. *Tetrahedron Lett.* **2001**, *42*, 7329.
- (6) Bharat; Bhola, R.; Bally, T.; Valente, A.; Cyranski, M. K.; Dobrzycki, Ł.; Spain, S. M.; Rempała, P.; Chin, M. R.; King, B. T. *Angew. Chem., Int. Ed.* **2010**, *49*, 399.
- (7) Dosche, C.; Löhmansröben, H.-G.; Bieser, A.; Dosa, P. I.; Han, S.; Iwamoto, M.; Schleifenbaum, A.; Vollhardt, K. P. C. *Phys. Chem. Chem. Phys.* **2002**, *4*, 2156 and references therein.

- (8) Trinajstić, N.; Schmalz, T. G.; Nikolić, S.; Hite, G. E.; Klein, D. J.; Seitz, W. A. *New J. Chem.* **1991**, *15*, 27.
- (9) (a) Blomquist, A. T.; Maitlis, P. M. *Proc. Chem. Soc. (London)* **1961**, 332. (b) Huntsman, W. D.; Wristers, H. J. *J. Am. Chem. Soc.* **1963**, *85*, 3308. (c) Huntsman, W. D.; Wristers, H. J. *J. Am. Chem. Soc.* **1967**, *89*, 342. (d) Collier, B. A. W.; Heffernan, M. L.; Jones, A. J. *Aust. J. Chem.* **1968**, *21*, 1807. (e) Hopf, H. *Angew. Chem., Int. Ed.* **1970**, *9*, 732. (f) Toda, F.; Garratt, P. *Chem. Rev.* **1992**, *92*, 1685.
- (10) (a) Fier, S.; Sullivan, R. W.; Rickborn, B. J. *Org. Chem.* **1988**, *53*, 2353. (b) Rainbolt, J. E.; Miller, G. P. *J. Org. Chem.* **2007**, *72*, 3020.
- (11) Kaupp, G.; Gruter, H.-W.; Teufel, E. *Chem. Ber.* **1983**, *116*, 618.
- (12) Simpson, J. H. *Organic Structure Determination Using 2-D NMR Spectroscopy*, 2nd ed.; Elsevier: Oxford, 2012; pp 137–139.
- (13) Sauer, J.; Sustmann, R. *Angew. Chem., Int. Ed.* **1980**, *19*, 779.
- (14) (a) Cava, M. P.; VanMeter, J. P. *J. Am. Chem. Soc.* **1962**, *84*, 2008. (b) Cava, M. P.; VanMeter, J. P. *J. Org. Chem.* **1969**, *34*, 538. (c) Mondal, R.; Shah, B. K.; Neckers, D. C. *J. Org. Chem.* **2006**, *71*, 4085.
- (15) (a) VanVeller, B.; Miki, K.; Swager, T. M. *Org. Lett.* **2010**, *12*, 1292. (b) Bowles, D. M.; Palmer, G. J.; Landis, C. A.; Scott, J. L.; Anthony, J. E. *Tetrahedron.* **2001**, *57*, 3753.
- (16) TIPS-anthracene was synthesized according to the procedure reported in the literature: Goldsmith, R. H.; Vura-Weis, J.; Scott, A. M.; Borkar, S.; Sen, A.; Ratner, M. A.; Wasielewski, M. R. *J. Am. Chem. Soc.* **2008**, *130*, 7659.
- (17) Roberts, S. T.; McAnally, R. E.; Mastron, J. N.; Webber, D. H.; Whited, M. T.; Brutchey, R. L.; Thompson, M. E.; Bradforth, S. E. *J. Am. Chem. Soc.* **2012**, *134*, 6388.
- (18) Holmes, D.; Kumaraswamy, S.; Matzger, A. J.; Vollhardt, K. P. C. *Chem.—Eur. J.* **1999**, *5*, 3399.